Mathematical and statistical modeling of morphometric and planar parameters of barchans in Pashoeyeh Erg in the west of Lut Desert, Iran

Hossein GHAZANFARPOUR[1], Mohsen POURKHOSRAVANI[1*], Sayed H MOUSAVI[2], Ali MEHRABI[3]

[1] Department of Geography and Urban Planning, Shahid Bahonar University of Kerman, Kerman 7618965984, Iran;
[2] Department of Geography and Ecotourism, Faculty of Natural Resources and Geosciences, University of Kashan, Kashan 8731753153, Iran;
[3] Department of Geography and Urban Planning, Shahid Bahonar University of Kerman, Kerman 7618965984, Iran

Abstract: Barchan dunes are among the most common accumulative phenomena made by wind erosion, which are usually formed in regions where the prevailing wind direction is almost constant throughout the year and there is not enough sand to completely cover the land surface. Barchans are among the most common windy landscapes in Pashoueyeh Erg in the west of Lut Desert, Iran. This study aims to elaborate on morphological properties of barchans in this region using mathematical and statistical models. The results of these methods are very important in investigating barchan shapes and identifying their behavior. Barchan shapes were mathematically modeled by simulating them in the coordinate system through nonlinear parabolic equations, so that two separate equations were calculated for barchan windward and slip-face parabolas. The type and intensity of relationships between barchan morphology and mathematical parameters were determined by the statistical modeling. The results indicated that the existing relationships followed the power correlation with the maximum coefficient of determination and minimum error of estimate. Combining the above two methods is a powerful basis for stimulating barchans in virtual and laboratory environments. The most important result of this study is to convert the mathematical and statistical models of barchan morphology to each other. Focal length is one of the most important parameters of barchan parabolas, suggesting different states of barchans in comparison with each other. As the barchan's focal length decreases, its opening becomes narrower, and the divergence of the barchan's horns reduces. Barchans with longer focal length have greater width, dimensions, and volume. In general, identifying and estimating the morphometric and planar parameters of barchans is effective in how they move, how much they move, and how they behave in the environment. These cases play an important role in the management of desert areas.

Keywords: barchan dunes; desert; parabolic equations; statistical model; wind erosion; Pashoueyeh Erg; Lut Desert

1 Introduction

The shape of aeolian sand dunes is determined by the directionality of the sand and wind

*Corresponding author: Mohsen POURKHOSRAVANI (E-mail: pourkhosravani@uk.ac.ir)
Received 2020-11-21; revised 2021-03-26; accepted 2021-03-28

availability (Cooke et al., 1993; Alvarez and Franklin, 2019). Basically, the wind can shape sand dunes by erosion and deposition processes (Hersen, 2005). When the sand supply is low and the wind is unidirectional or flat, crescentic dunes which are called barchans appear and move along the wind direction (Engel et al., 2018). Barchans have a crescent-shaped morphology with two horns pointing in the wind direction (Zhang et al., 2018). Barchans observed in nature are found in many different sizes. These crescent-shaped dunes are usually display an asymmetric shape with the width larger than the length (Tsoar and Parteli, 2016). In the process of transformation and evolution of barchan dunes, it is assumed that the initial accumulation of sands forms parabolic dunes. If the height of parabolic dunes reaches a certain critical value, their appearance looks instable and a slippery mass is formed on the barchan slip-face. As the height increases, the dune becomes more stable (Kocurek et al., 1992). However, barchan dunes continue to grow and move (Sauermann et al., 2000). During the movements and transformations, these dunes maintain their parabolic and three-dimensional shape along with increasing the volume and size until they reach complete stability. In general, each barchan is composed of the intersection of three separate parabolas with different characteristics. Each parabola individually has a focus, vertex, directrix, and separate equation. The first or outer parabola indicates the maximum expansion of the windward slope, the middle or second parabola represents the barchan's brink, and the third parabola indicates the maximum expansion of the leeward slope. Parabola is a set of points in a plane that are equidistant from a fixed point, called focus, and a fixed line, called directrix (Leithold, 1992). Nature barchans show various forms of geometric shapes, and the appearance and morphology of which can be modeled in mathematics through linear and nonlinear functions and mathematical equations. Barchan dunes are real manifestations of parabolic geometric shapes, to which the mathematical rules of parabola can be applied, and their appearance can be modeled through nonlinear functions and parabolic equations. This analogy helps researchers better identify these phenomena and their performance in the nature and accurately understand their behavior in management based on the systemic approach of desert areas. Barchan mathematical modeling using parabolic equations helps to determine the exact area under the parabolic curve, which can be used to calculate surface components of barchans such as environment and area.

Morphometric calculations of barchan dunes and the morphological relationships between them were first performed by Bagnold (1941) and Finkel (1959) in southern Peru. Lettau and Lettau (1969) also developed a simple geometric pattern consisting of elliptical and parabolic shapes and straight lines to stimulate a standard barchan dune using the height, width, and length of the barchan and calculated the volume of sand dunes. In general, many researchers have used numerical simulations to predict the movement and evolution of barchans dunes and their morphology (Landsberg, 1956; Howard and Morton, 1978; Anton and Vincent, 1986; Wippermann and Gross, 1986; Anthonsen et al., 1996; Sauermann et al., 2000; Hersen, 2004; Mousavi et al., 2010; Durán et al., 2011; Hamdan et al., 2016; Yang et al., 2019). Also, Hesp and Hastings (1998), by examining the relationships between the morphological parameters of barchans, introduced these relationships as factors controlling the three-dimensional shape of barchans. Sauermann et al. (2000) studied barchan dunes in southern Morocco using three-dimensional parabolic equations and proposed a model for the barchan shape based on which the differences between barchans and their stability can be defined. Wang et al. (2007) investigated barchan dunes in northwestern China through geometric theories and stated that the barchan height was proportional to its width and the brink can be described by a parabolic shape. Also, Zhang et al. (2018) studied the migration and morphology of asymmetric barchans in Northwest China, and the results showed that morphometric relations that are predicted from models for steady-state, symmetric crescent-shaped dunes can be applied to different transitional morphologies of interacting, asymmetric barchans.

The present study aims to investigate the morphometric and planar features of barchan dunes in the selected region using mathematical modeling, quantitative measurement methods, and parabolic equations. This study presents quadratic equations for barchan parabolas to better identify their behavior, performance, and morphometric and planar properties in the nature.

Therefore, barchans' horizontal sections are first examined to see if they follow parabolic equations and, then, the components of these equations are modeled using geometric properties of barchans. A combination of statistical and mathematical modeling is employed to study the shape of barchans. These equations are useful for defining the morphometric and planar indices of barchans, simulating them in virtual and laboratory environments, and accurately identifying their behavior and morphodynamic features.

2 Materials and methods

2.1 Study area

The Pashoeyeh Erg is located in the west of Lut Desert, eastern part of Kerman Province, Iran. It is situated along the northwest-southeast in the east of Kalouts of Lut Desert, with the elevation of 970 m above the sea level. The field under this study (Pashoeyeh Erg) is situated between latitudes 29°55′–30°21′N and longitudes 57°50′–58°10′E. Lut Desert is one of the most important deserts in Iran. This desert is among the driest and hottest deserts in Iran and in the world, with an annual precipitation of less than 50 mm; it is likely that no rain falls there even for several consecutive years. Table 1 shows the characteristics of climatic parameters in the study area.

Table 1 Monthly average of climatic parameters in the study area (2003–2019)

Month	Precipitation (mm)	Temperature (°C)	Humidity (%)
Jan	6.40	13.70	36.90
Feb	9.90	17.30	33.80
Mar	8.50	23.60	26.80
Apr	1.50	29.90	23.30
May	1.20	30.10	17.40
Jun	0.20	40.10	12.80
Jul	0.00	41.20	12.00
Aug	0.00	39.20	12.30
Sept	0.00	35.40	13.30
Oct	0.00	29.80	15.20
Nov	1.20	21.10	24.60
Dec	3.30	14.90	31.70

According to the results of Table 1, in the four months of the year, i.e., July, August, September, and October, there was no rainfall in the study area. Accordingly, the highest precipitation in February was 9.90 mm. Also, July with an average temperature of 41.20°C was the warmest month and January with an average temperature of 13.70°C was the coldest month in this region. The highest humidity was 36.90% in January and the lowest was 12.00% in July. The analysis of the wind-rose diagram of Shahdad synoptic station in the northwest of the study area shows that the prevailing wind direction in the study area is from north (data not shown). The maximum wind speed in this direction is 11.11 m/s.

2.2 Parameter measurements and data analysis

The study area was investigated by using satellite images of Google Earth. Field sampling was performed along ten transects that covered almost the entire study area and morphometric and planar parameters of barchans were measured along each transect (Table 2). The sample size depends on the number of barchans located in the area of transects. In total, 50 barchans were evaluated. In other words, based on field sampling, 50 barchans overlapped with the ten mentioned transects.

Morphometric and planar parameters of barchans were measured to statistically investigate their characteristics. Figure 1 shows morphometric and planar parameters of barchans and the way they were measured.

Table 2 Morphometric and planar parameters of barchans in the study area

Sample barchan	Length (m)	Width (m)	Perimeter (m)	Area ($\times 10^3$ m^2)	Height (m)	Volume ($\times 10^3$ m^3)
Barchan 1	270.25	290.13	605.45	8.81	3.10	4.55
Barchan 2	156.51	185.95	649.96	19.66	3.50	11.47
Barchan 3	220.45	235.25	555.18	8.76	2.60	3.80
Barchan 4	737.88	1100.02	4632.54	190.54	9.00	285.69
Barchan 5	154.69	153.37	613.25	15.22	3.30	8.37
Barchan 6	570.35	840.85	3800.25	173.76	8.20	237.37
Barchan 7	177.56	164.13	631.61	18.35	3.30	10.09
Barchan 8	350.15	355.32	900.52	28.71	4.80	22.96
Barchan 9	674.54	946.72	3912.14	173.89	8.60	249.15
Barchan 10	450.55	600.35	3580.65	13.65	7.40	16.83
Barchan 11	180.71	193.63	746.80	17.99	3.00	8.99
Barchan 12	196.63	196.87	710.21	25.98	3.30	14.28
Barchan 13	100.85	110.45	430.65	8.60	2.50	3.58
Barchan 14	735.97	879.93	3824.34	138.15	8.10	186.43
Barchan 15	150.22	160.85	600.95	17.56	2.80	8.19
Barchan 16	110.86	120.82	440.21	8.61	2.60	3.73
Barchan 17	155.21	168.48	593.51	17.53	2.60	7.60
Barchan 18	190.35	210.68	780.45	25.39	3.20	13.54
Barchan 19	790.19	776.33	3349.39	134.97	7.60	170.89
Barchan 20	125.64	115.93	476.11	7.75	2.00	2.59
Barchan 21	125.15	140.35	514.91	10.98	2.00	3.66
Barchan 22	210.23	220.56	540.24	8.71	2.70	3.92
Barchan 23	300.25	308.55	860.45	28.66	4.50	21.48
Barchan 24	183.13	196.32	720.93	24.71	2.50	10.29
Barchan 25	815.94	722.44	3250.63	119.11	7.00	138.90
Barchan 26	159.91	155.87	602.39	15.38	3.30	8.46
Barchan 27	161.91	158.87	605.39	15.38	3.50	8.97
Barchan 28	160.52	190.95	651.96	19.67	3.70	12.12
Barchan 29	198.95	209.66	782.51	28.54	4.10	19.50
Barchan 30	699.91	1111.12	4644.49	189.99	8.90	281.71
Barchan 31	149.98	150.95	609.97	15.20	3.50	8.87
Barchan 32	210.81	212.53	789.28	28.55	4.00	19.03
Barchan 33	180.25	168.52	638.12	18.36	3.70	11.32
Barchan 34	200.15	215.65	790.15	27.19	4.00	18.12
Barchan 35	595.55	895.75	3850.88	173.80	7.80	225.85
Barchan 36	150.12	165.58	570.65	14.76	3.50	8.61
Barchan 37	195.15	211.51	783.34	27.18	3.60	16.30
Barchan 38	170.75	183.63	735.85	18.18	3.10	9.39
Barchan 39	180.75	181.88	690.95	25.86	3.00	12.93
Barchan 40	600.85	750.25	3725.95	13.80	7.80	17.93
Barchan 41	140.47	159.91	560.54	14.64	3.00	7.32
Barchan 42	120.52	130.65	450.53	8.76	2.80	4.09
Barchan 43	150.25	170.35	605.57	17.66	3.20	9.41
Barchan 44	90.46	100.85	420.45	8.59	2.20	3.15
Barchan 45	180.95	200.93	775.25	25.37	3.10	13.11
Barchan 46	183.91	203.02	768.23	25.36	3.00	12.68
Barchan 47	750.65	736.55	3295.95	135.13	7.50	168.84
Barchan 48	120.85	110.95	460.76	7.69	2.40	3.08
Barchan 49	130.15	150.21	525.15	11.06	2.30	4.24
Barchan 50	170.45	180.54	620.95	24.61	2.20	9.02

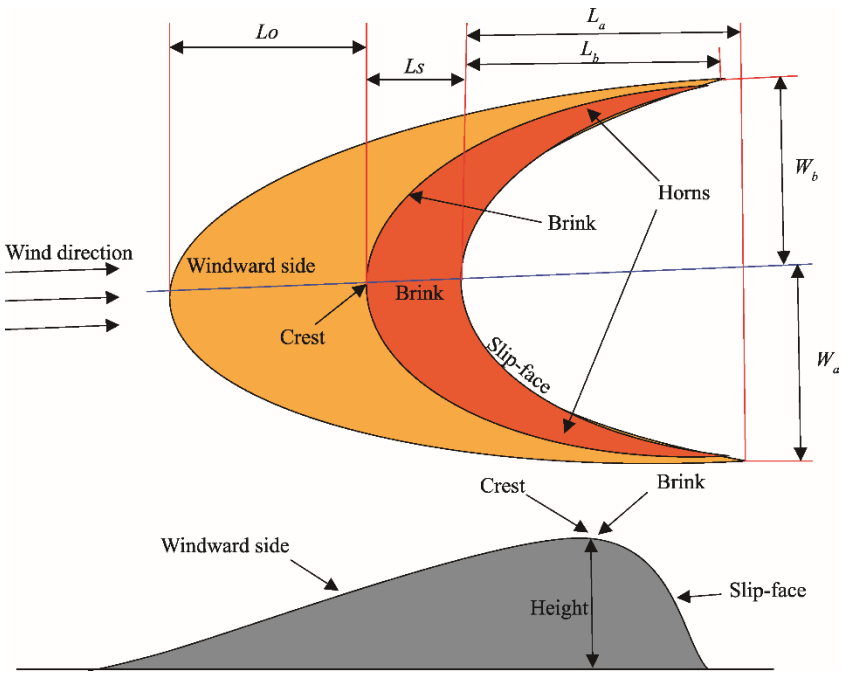

Fig. 1 A schematic representation of barchan's morphometric and planar parameters (Hesp ans Hastings, 1998; Sauermann et al., 2000; Daniell and Hughe, 2007). *Lo*, length of the windward side; *Ls*, length of the slip-face; L_a, length of the right horn; L_b, length of the left horn; W_a, width of the right side; W_b, width of the left side. The yellow color indicates the windward side, the orange color indicates the slip-face of the barchan, and the gray color indicates the barchan.

The total length and width of barchans were calculated using Equations 1 and 2, respectively:

$$L = Lo + Ls + \frac{(L_a + L_b)}{2}, \quad (1)$$

$$W = W_a + W_b, \quad (2)$$

where L is the total length of the barchans (m); L_a is the length of the right horn (m); L_b is the length of the left horn (m); Lo is the length of the windward side (m); Ls is the length of the slip-face (m); W is the total width of the barchan (m); W_a is the width of the right side (m); and W_b is the width of the left side (m).

To calculate the perimeter and area of the barchan, we first considered a hypothetical coordinate system for each barchan on the ground. Then, coordinates of 21 points were determined on its perimeter. The sampled points were plotted on a graph paper at a scale of 1:100. Then, the area and perimeter of each barchan were calculated using a planimeter and curvimeter, respectively. Considering that the barchan's volume was half of the pyramid's volume (Hesse, 2008), we determined the volume of sediments using Equation 3 after calculating the barchan's area.

$$V = 0.1666S \times H, \quad (3)$$

where V is the volume of the barchan (m^3); and S and H are the area (m^2) and height (m) of the barchan, respectively. The volumes of all the barchans were calculated and, finally, the volume vector of the barchan was formed. Therefore, the height, length and its parameters, width and its parameters, perimeter, area, and volume of wind-eroded sediments were calculated for all the 50 barchans, and data matrices were prepared for modeling.

To model the studied barchan parabolas, we selected 20 barchans out of the 50-member population of barchans using the probability sampling method (simple random sampling). Then, based on the 21 points selected on the ground, we plotted these 20 barchans on a graph paper at a scale of 1:100. To mathematically model them using the parabolic equation, we plotted a

hypothetical coordinate system for each of the barchans, the *x*-axis and *y*-axis of which were parallel to the wind direction and perpendicular to the wind direction, respectively. The coordinate system was plotted in such a way that the barchan's opening and its parabolas were placed on the right side. In this coordinate system, the *x*-axis corresponded to the symmetry line of the barchan and windward, so that the coordinates of the vertex of the windward slope parabola also corresponded to the origin of the coordinate system (Fig. 2). Then, by grading the axes of the coordinate system in millimeter at a scale of 1:100, the coordinates of the end points of the barchan's horns were determined. Finally, given that parabolas opened to the right, the barchan windward slope parabola was modeled using the following parabola equation:

$$y^2 = 4p(x). \tag{4}$$

In this equation, $4p$ is the length of the side perpendicular to the parabola's focus, and x and y are the length and width of the constituent points of parabolas, respectively. This equation is applied when the parabola's vertex is located at coordinates (0, 0), i.e., in the center of the coordinate system. In this case, the focus has coordinates (0, p), the directrix equation is $x = -p$, and the parabola's symmetry line is the *x*-axis. Considering the coordinate system described, these conditions indicated the barchan windward slope parabola whose equation can be easily calculated (Fig. 2).

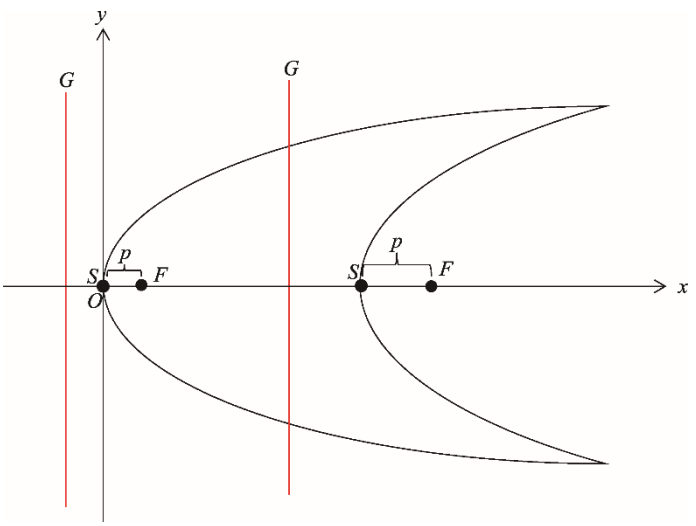

Fig. 2 Image of a barchan with its parabolas and components in the coordinate system. In this image, *O* is the origin of the coordinate system, *F* is the coordinates of the focus, *S* is the coordinates of the parabola's vertex, *p* is the distance between the focus and vertex, and *G* is the directrix of the parabola.

The barchan slip-face slope parabola was also modeled in the same coordinate system by transferring the axis to the vertex of the barchan slip-face parabola using Equation 5; however, this equation was based on the coordinate system, and the origin of which was the vertex of the windward slope parabola (Fig. 2).

$$(y-k)^2 = 4p(x-h), \tag{5}$$

where h is the vertex of the slip-face parabola; and k is the vertex of the slip-face parabola.

This equation is applicable when the parabola's vertex has coordinates other than (0, 0). In this case, the axis should be transferred to calculate the parabolic equation. Therefore, according to its length and width (i.e., k and h, respectively), h is subtracted from x and k is subtracted from y in the parabolic equation. In this way, the axis was transferred and the leeward slope parabolic equation was calculated. Finally, Equation 4 became Equation 5, representing that the vertex of the leeward parabola is located at a point with coordinates (k, h) and the equation is h units away from the *x*-axis and k units away from the *y*-axis in the positive direction.

In this case, the coordinates of the parabola's focus were calculated by the following equation:

$F(h+p, k)$, where F is the coordinates of the focus, p is the distance between the focus and vertex, and the directrix equation was obtained by $x=h–p$. Using this method, the equation of barchan slip-face parabola and other related properties can be modeled. Given that the vertex of the windward slope parabola corresponds to the vertex of the axis of the coordinates, h and k values are equal to zero. However, these values are different in the slip-face parabola, because its vertex is located on the x-axis and away from the y-axis, so that k value is equal to zero and h value is equal to its distance from the y-axis (Fig. 2).

Overall, the coordinates of the parabola's vertex and the end points of the horns were determined for all the 20 barchans studied, and the parabolic equations, coordinates of the focus, directrix equation, and p values were calculated for each of them. After modeling the studied barchan parabolas mathematically and calculating p values and coefficient x to identify the type of relationship and the extent of effect of these two parameters on the morphometric and planar parameters of barchans, the relationship between these parameters was evaluated using SPSS software and regression analysis. For this purpose, simple linear and nonlinear regression methods were first tested. In simple regression method, various relationships including linear, power, logarithmic, and cubic were assessed among different parameters and those with higher preference value (higher coefficient of determination and lower standard error of estimate) were selected. In other words, in this method, the best relationships are those that follow power functions.

Therefore, only simple power correlations are mentioned in the following section and, finally, correlation coefficient, coefficient of determination, adjusted coefficient of determination, standard error of estimate, and significance level of relationships are presented to identify the type of relationship and the extent of its impact.

3 Results and discussion

The study area was located in the west of Lut Desert, where many barchan dunes can be found. Table 3 shows the statistical characteristics of the studied samples in the study area. As can be seen in this table, the maximum and minimum heights of barchans were 9.00 and 2.00 m, respectively. Also, the maximum and minimum lengths of barchans were 815.94 and 110.87 m, respectively. The maximum and minimum widths of barchans were 1100.02 and 115.93 m, respectively.

Table 3 Statistical characteristics of the studied barchans in the study area

Parameter	Minimum	Maximum	Difference	Mean	SD	Skewness
Length (m)	110.87	815.94	705.07	310.64	263.21	1.250
Width (m)	115.93	1100.02	984.09	350.36	325.10	1.393
Perimeter (m)	440.20	4632.54	4192.34	1428.70	1426.79	1.355
Area (m^2)	7747.12	191,000.00	183,000.00	51,723.00	60,823.68	1.407
Height (m)	2.00	9.00	7.00	4.27	2.33	1.166
Volume (m^3)	2582.27	286,000.00	283,000.00	58,838.00	91,642.22	1.578

Note: SD, standard deviation.

The parabolic shape is among the most important morphometric and planar properties of barchans, which is itself influenced by barchan's crescent and aerial morphology (Sauermann et al., 2000). Therefore, parabolic quadratic equations can be used for mathematical modeling of barchans. In other words, it is possible to model two-dimensional surfaces of barchans (regardless of their spatial features) through parabolic equations (Anthonsen et al., 1996). For mathematical modeling of barchans, the coordinate system was designed in a way that barchan parabolas opened to the right in the wind direction. The vertex of the windward slope parabola corresponded to the origin of the coordinate system and the x-axis was parallel to the wind direction and the symmetry line of barchans. Therefore, the coordinates of the vertex and the

focus of parabolas were positive, and their values in the coordinates of the focus and vertexes of all barchan parabolas were constant.

However, the p value and coefficient x in the equation of each barchan were different from the adjacent barchans. Directrix in all barchans was parallel to the y-axis. The p value or the focal length of the parabola and the value of coefficient x in the parabolic equation are among the important parameters in calculating the parabolic equation of a barchan dune to study its morphology. These two components represent different states of parabolas, so that as the p value decreases, the focal length and the value of coefficient x also reduce. As a result, as these values decrease, the focus becomes closer to the vertex; the barchan's opening narrows and, consequently, the divergence of the barchan's horns decreases. In the other case, the opposite happens.

In a barchan consisting of three separate parabolas, the windward slope parabola has a lower p value, and this value increases in the other two parabolas, i.e., the windward slope parabola has the lowest p value and the slip-face parabola has the highest p value. As a result, the degree of divergence of parabolic horns increases from the windward slope to the slip-face with increasing p value and coefficient x. Therefore, the windward slope parabola has the lowest degree of divergence compared to the slip face parabola, and the slip-face parabola has the highest degree of divergence. In barchan dunes, the longer the distance between the focus and vertex is, the greater the barchan's focal length and width will be. If the opposite happens, the barchan's width decreases and its length increases, which changes its shape. In general, barchans with longer focal length have greater width, dimensions, and volume.

Table 4 shows the results of mathematical modeling of the studied barchans using parabolic equations, in which p value, directrix equation, parabolic equation, coordinates of the focus, and coordinates of the vertex are presented. Table 5 presents the correlations between the focal length of the windward slope parabola and the morphometric and planar parameters of barchans in the study area.

The analysis of the correlation between the focal length of the windward slope parabola and other morphometric and planar parameters of the barchan indicated that there was a maximum significant power correlation of the focal length of the windward slope parabola with the barchan's area and volume, with the coefficients of determination of 0.989 and 0.984, respectively, and the estimation errors of 0.148 and 0.250, respectively (Table 5). Next to the parameters of area and volume, the width of the barchan had the third highest correlation with the focal length, with the coefficient of determination of 0.970 and the estimation error of 0.156. Also, the minimum significant power correlation was observed between the focal length of the windward slope parabola and the barchan's length, with a coefficient of determination of 0.952 and an estimation error of 0.311 (Fig. 3). Next to the length parameter, the perimeter of the barchan had the second least correlation with the focal length, with the coefficient of determination of 0.957 and the estimation error of 0.247.

The analysis of the correlation between the focal length of the slip-face parabola and other morphometric and planar parameters of the barchan indicated that there was a maximum significant power correlation of the focal length of the slip-face parabola and the barchan's width and area, with the coefficients of determination of 0.797 and 0.785, respectively, and the estimation errors of 0.497 and 0.650, respectively (Table 6).

Next to the parameters of area and width, the volume of the barchan had the third highest correlation with the focal length of the slip-face parabola with the coefficients of determination of 0.772 and the estimation errors of 0.934. Also, the minimum significant power correlation was observed between the focal length of the slip-face parabola and the barchan's length, with a coefficient of determination of 0.705 and an estimation error of 0.887. Next to the length parameter, the height of the barchan had the second least correlation with the focal length of the slip-face parabola, with the coefficient of determination of 0.732 and the estimation errors of 0.288 (Fig. 4).

Table 4 Results of mathematical modeling of the studied barchans in the study area using parabolic equations

Samples for modeling barchan parabolas	Parabola	p (m)	Coordinates of the vertex	Equation of the directrix	Coordinates of the focus	Parabola equation
Barchan 1	Windward side	15.45	0.00, 0.00	x= –15.45	15.45, 0.00	y^2=61.798x
	Slip-face	11.60	91.46, 0.00	x=79.86	103.07, 0.00	y^2=46.42(x–91.46)
Barchan 2	Windward side	16.56	0.00, 0.00	x= –16.56	16.56, 0.00	y^2=66.260x
	Slip-face	22.84	129.11, 0.00	x=106.27	151.95, 0.00	y^2=91.36(x–129.11)
Barchan 3	Windward side	19.59	0.00, 0.00	x= –19.59	19.59, 0.00	y^2=78.350x
	Slip-face	16.12	135.82, 0.00	x=119.69	151.94, 0.00	y^2=64.48(x–135.82)
Barchan 4	Windward side	30.87	0.00, 0.00	x= –30.87	30.87, 0.00	y^2=123.501x
	Slip-face	42.15	295.19, 0.00	x=253.04	337.33, 0.00	y^2=168.61(x –295.19)
Barchan 5	Windward side	18.12	0.00, 0.00	x= –18.12	18.12, 0.00	y^2=72.470x
	Slip-face	9.05	82.49, 0.00	x=73.44	91.54, 0.00	y^2=36.20(x–82.49)
Barchan 6	Windward side	17.85	0.00, 0.00	x= –17.85	17.85, 0.00	y^2=71.390x
	Slip-face	23.43	107.12, 0.00	x=83.69	130.55, 0.00	y^2=93.73(x–107.12)
Barchan 7	Windward side	16.74	0.00, 0.00	x= –16.74	16.74, 0.00	y^2=66.980x
	Slip-face	17.31	134.01, 0.00	x=116.71	151.32, 0.00	y^2=69.23(x–134.012)
Barchan 8	Windward side	29.82	0.00, 0.00	x= –29.83	29.83, 0.00	y^2=119.304x
	Slip-face	42.86	291.33, 0.00	x=248.47	334.20, 0.00	y^2=171.45(x–291.33)
Barchan 9	Windward side	16.80	0.00, 0.00	x= –16.80	16.80, 0.00	y^2=67.208x
	Slip-face	9.33	107.83, 0.00	x=98.49	117.17, 0.00	y^2=37.34(x–107.83)
Barchan 10	Windward side	15.31	0.00, 0.00	x= –15.37	15.37, 0.00	y^2=61.470x
	Slip-face	21.97	110.12, 0.00	x=88.15	132.09, 0.00	y^2=87.89(x–110.12)
Barchan 11	Windward side	23.44	0.00, 0.00	x= –23.44	23.44, 0.00	y^2=93.750x
	Slip-face	35.05	145.14, 0.00	x=110.08	180.19, 0.00	y^2=140.21(x–145.14)
Barchan 12	Windward side	38.55	0.00, 0.00	x= –38.55	38.55, 0.00	y^2=154.197x
	Slip-face	51.55	237.40, 0.00	x=185.85	288.94, 0.00	y^2=206.19(x–237.397)
Barchan 13	Windward side	12.11	0.00, 0.00	x= –12.11	12.11, 0.00	y^2=48.440x
	Slip-face	9.86	75.95, 0.00	x=66.08	85.81, 0.00	y^2=39.45(x–75.95)
Barchan 14	Windward side	14.10	0.00, 0.00	x= –14.10	14.10, 0.00	y^2=56.420x
	Slip-face	17.73	114.15, 0.00	x=96.41	131.88, 0.00	y^2=70.93(x–114.15)
Barchan 15	Windward side	21.50	0.00, 0.00	x= –21.50	21.50, 0.00	y^2=85.990x
	Slip-face	25.08	128.38, 0.00	x=103.30	153.45, 0.00	y^2=100.31(x–128.38)
Barchan 16	Windward side	51.52	0.00, 0.00	x= –51.52	51.52, 0.00	y^2=206.091x
	Slip-face	64.75	195.17, 0.00	x=130.42	259.93, 0.00	y^2=259.012(x–195.17)
Barchan 17	Windward side	12.39	0.00, 0.00	x= –12.39	12.39, 0.00	y^2=49.560x
	Slip-face	17.46	60.93, 0.00	x=43.47	78.40, 0.00	y^2=69.85(x–60.93)
Barchan 18	Windward side	13.23	0.00, 0.00	x= –13.24	13.24, 0.00	y^2=52.940x
	Slip-face	8.69	83.08, 0.00	x=74.39	91.77, 0.00	y^2=34.76(x–83.08)
Barchan 19	Windward side	19.09	0.00, 0.00	x= –19.09	19.09, 0.00	y^2=76.370x
	Slip-face	18.72	130.46, 0.00	x=111.74	149.18, 0.00	y^2=74.88(x–130.46)
Barchan 20	Windward side	57.27	0.00, 0.00	x= –57.27	57.27, 0.00	y^2=229.870x
	Slip-face	72.22	188.11, 0.00	x=115.89	260.33, 0.00	y^2=288.88(x–188.108)

Table 5 Correlations between the focal length of the windward slope parabola and the morphometric and planar parameters of barchans in the study area

Parameters	Type of relationship	r	R^2	R^2_{adj}	SE	Sig.
Focal length & width	Power	0.985	0.970	0.955	0.156	0.015
Focal length & length	Power	0.976	0.952	0.929	0.311	0.024
Focal length & height	Power	0.981	0.962	0.943	0.109	0.190
Focal length & perimeter	Power	0.978	0.957	0.935	0.247	00.22
Focal length & area	Power	0.994	0.989	0.983	0.148	0.006
Focal length & volume	Power	0.992	0.984	0.975	0.250	0.008

Note: r, correlation coefficient; R^2, coefficient of determination; R^2_{adj}, adjusted coefficient of determination; SE, standard error of estimate; Sig., significance level.

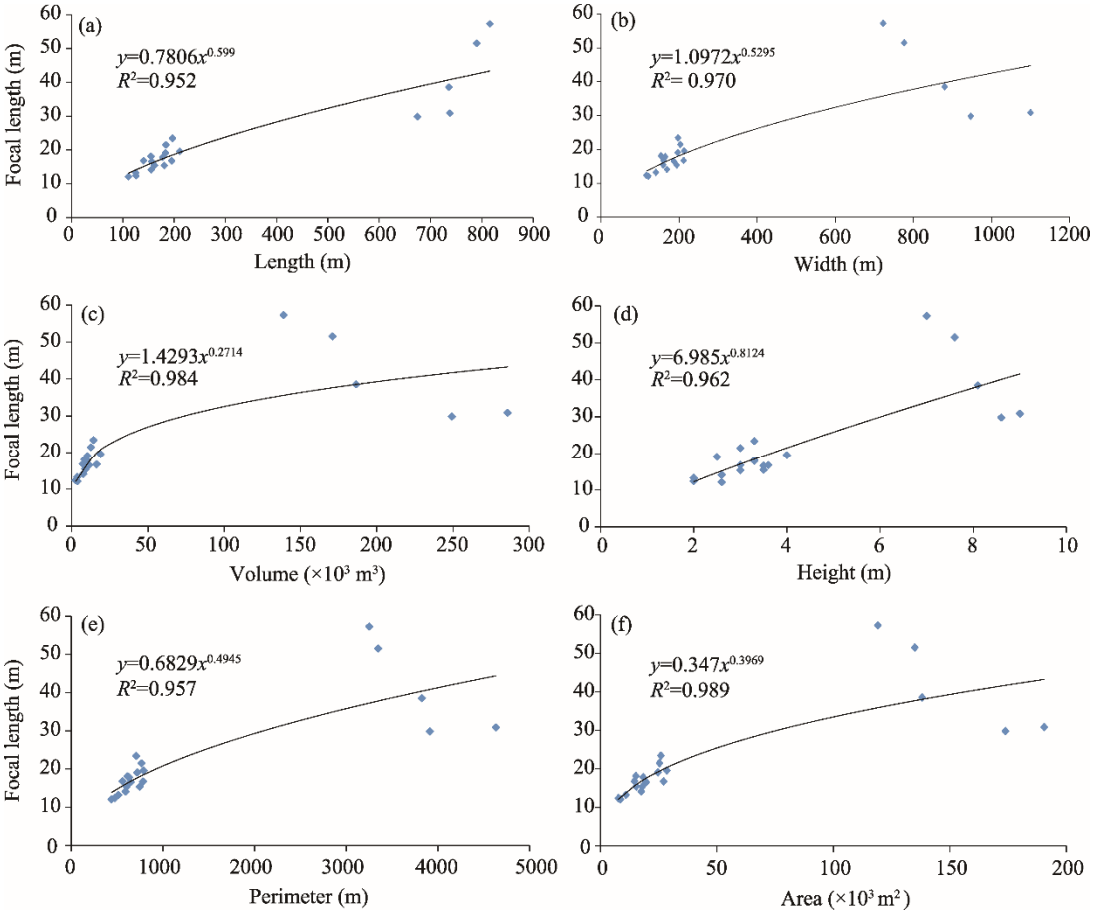

Fig. 3 Relationships between the focal length of windward slope parabola and the morphometric and planar parameters of barchans in the study area. (a), length; (b), width; (c), volume; (d), height; (e), perimeter; (f), area.

Table 6 Correlations between the focal length of the slip-face parabola and the morphometric and planar parameters of barchans in the study area

Parameters	Type of relationship	r	R^2	R^2_{adj}	SE	Sig.
Focal length & width	Power	0.893	0.797	0.695	0.497	0.107
Focal length & length	Power	0.840	0.705	0.558	0.887	0.160
Focal length & height	Power	0.856	0.732	0.599	0.288	0.144
Focal length & perimeter	Power	0.874	0.763	0.645	0.577	0.126
Focal length & area	Power	0.886	0.785	0.677	0.650	0.114
Focal length & volume	Power	0.878	0.772	0.657	0.934	0.122

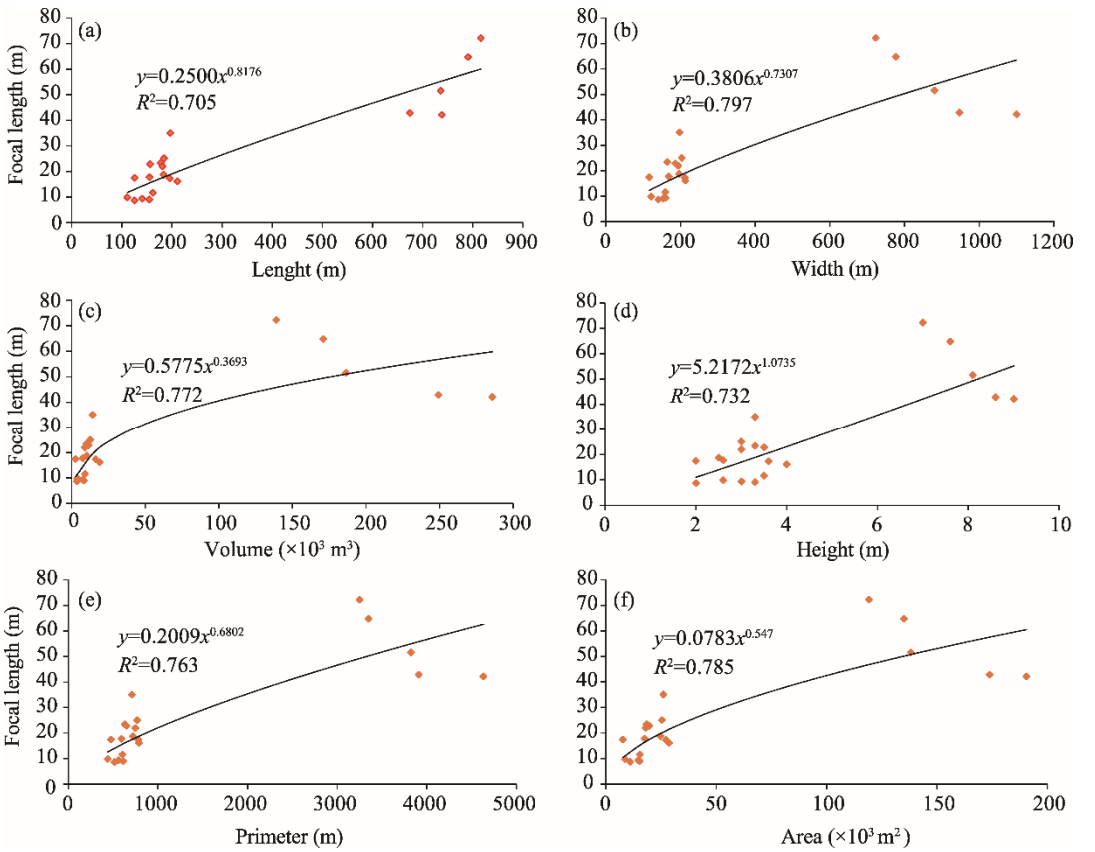

Fig. 6 Relationships between the focal length of slip-face parabola and the morphometric and planar parameters of barchans in the study area. (a), length; (b), width; (c), volume; (d), height; (e), perimeter; (f), area.

Table 7 indicates the correlation coefficients between the focal length of the windward slope parabola and the morphometric and planar parameters of barchans in the study area as well as the significance level of the coefficients of the equations. The results show that the correlation between the focal length of the windward slope parabola and the volume of the barchan exhibited the lowest estimation errors of 0.010; and, the correlation between the focal length of the windward slope parabola and the area of the barchan had the highest standard error of 0.542.

Table 7 Correlations between the focal length of the windward slope parabola and the morphometric and planar parameters of barchans in the study area

Parameters	Equation parameter	Unstandardized coefficient	SE	*t*	Sig.	Equation
Focal length & width	Constant	0.061	0.075	0.814	0.501	$p=0.061W^{2.843}$
	Power	2.834	0.410	6.917	0.020	
Focal length & length	Constant	0.247	0.210	1.176	0.361	$p=0.247L^{2.317}$
	Power	2.317	0.283	8.176	0.150	
Focal length & height	Constant	0.064	0.038	1.656	0.240	$p=0.64H^{0.124}$
	Power	1.431	0.201	7.109	0.019	
Focal length & perimeter	Constant	0.124	0.171	0.729	0.542	$p=0.124P^{3.041}$
	Power	3.041	0.457	6.647	0.022	
Focal length & area	Constant	0.658	0.542	1.214	0.349	$p=0.658A^{3.650}$
	Power	3.650	0.275	13.297	0.006	
Focal length & volume	Constant	0.007	0.010	0.718	0.547	$p=0.007V^{5.081}$
	Power	5.081	0.464	10.947	0.008	

Note: *t*, *t*-statistic; *p*, the distance between the focus and vertex; *W*, width; *L*, length; *H*, height; *P*, perimeter; *A*, area; *V*, volume.

Table 8 presents the correlation coefficients between the focal length of the slip-face parabola and the morphometric and planar parameters of barchans in the study area as well as the significance level of the coefficients of the equations. The results show that the correlation between the focal length of the slip-face parabola and the height of the barchan had the lowest estimation error of 0.301; and, the correlation between the focal length of the slip-face parabola and the area of the barchan exhibited the highest standard error of 288.796. The results indicated that a good linear relationship exhibited between the height of slip-face parabola and the width of horns (Hesp and Hastings, 1998; Sauermann et al., 2000).

Table 8 Correlation coefficients between the focal length of the slip-face parabola and the morphometric and planar parameters of barchans in the study area

Parameters	Equation parameter	Unstandardized coefficient	SE	*t*	Sig.	Equation
Focal length & width	Constant	3.507	5.592	0.627	0.595	$p=3.507W^{1.457}$
	Power	1.457	0.521	2.799	0.107	
Focal length & length	Constant	8.589	13.402	0.641	0.587	$p=8.589L^{1.115}$
	Power	1.115	0.509	2.189	0.160	
Focal length & height	Constant	0.543	0.501	1.084	0.392	$p=0.543H^{0.705}$
	Power	0.705	0.301	2.340	0.144	
Focal length & perimeter	Constant	10.600	19.605	0.541	0.643	$p=10.600P^{1.533}$
	Power	1.533	0.604	2.539	0.126	
Focal length & area	Constant	138.689	288.796	0.480	0.678	$p=138.689A^{1.836}$
	Power	1.836	0.680	2.700	0.114	
Focal length & volume	Constant	12.553	37.580	0.334	0.770	$p=12553V^{2.541}$
	Power	2.541	0.977	2.599	0.122	

4 Conclusions

In this study, two statistical and mathematical modeling methods were combined to investigate the morphometric and planar parameters of barchan dunes. The planar coordinates of barchan's parameters can be obtained using parabolic equation, mathematical modeling of barchans, and the intersection of two windward slope and slip-face parabolas. The morphometric and planar parameters of barchans can be calculated through statistical modeling of their geometric properties, and their properties can be justified by regression analysis. Therefore, the results of this study provide the possibility for accurate and rapid estimation of the morphometric and planar parameters of barchans. The evaluation of the focal length in the studied barchans shows that the maximum and minimum focal lengths in the sampled barchans are 72.22 and 8.69 m, respectively. The results of correlation analysis between the focal length and the morphometric and planar parameters of barchans indicate that, the focal length of the windward side parabola and the area of the barchan shows the highest correlation, with the coefficient of determination being of 0.989 and the estimation error of 0.148; while the length of the barchan has the least correlation with the focal length of the windward side parabola, with the coefficient of determination being of 0.952 and the estimation error of 0.311. The results of this simulation are of great significance for calculating the area of barchans under the curve and the perimeter and area occupied by the barchans in the nature.

References

Alvarez C A, Franklin E M. 2019. Horns of subaqueous barchan dunes: A study at the grain scale. Physical Review E, 100(4): 042904, doi: 10.1103/PhysRevE.100.042904.

Anton D, Vincent P. 1986. Parabolic dunes of the Jafurah Desert, Eastern Province, Saudi Arabia. Journal of Arid Environments, 11(3): 187–198.

Anthonsen K L, Clemmensen L B, Jensen J H. 1996. Evolution of a dune from crescentic to parabolic form in response to

short-term climatic changes: Rabjerg Mile, Skagen Odde, Denmark. Geomorphology, 17(1–3): 63–77.

Bagnold R A. 1941. The Physics of Blown Sand and Desert Dunes. London: Methuen Press, 232.

Cooke R, Warren A, Goudie A. 1993. Desert Geomorphology. London: UCL Press, 325.

Daniell J, Hughes M. 2007. The morphology of barchan-shaped sand banks from western Torres Strait, northern Australia. Sedimentary Geology, 202(4): 638–652.

Durán O, Schwämmle V, Lind P G, et al. 2011. Size distribution and structure of Barchan dune fields. Nonlinear Processes in Geophysics, 18(4): 455–467.

Engel M, Boesl F, Brückner H. 2018. Migration of barchan dunes in qatar–controls of the shamal, teleconnections, sea-level changes and human impact. Geosciences, 8(7): 240, doi: 10.3390/ geosciences8070240.

Finkel H J. 1959. The barchans of Southern Peru. Journal of Geology, 67(6): 614–647.

Hamdan M A, Refaat A A, Abdel Wahed M. 2016. Morphologic characteristics and migration rate assessment of barchan dunes in the Southeastern Western Desert of Egypt. Geomorphology, 257: 57–74.

Hersen P. 2004. On the crescentic shape of barchan dunes. The European Physical Journal, 37(4): 507–514.

Hersen P. 2005. Flow effects on the morphology and dynamics of Aeolian and subaqueous barchan dunes. Journal of Geophysical Research, 110(F4): 2–10.

Hesp P A, Hastings K. 1998. Width, height and slope relationships and aerodynamic maintenance of barchans. Geomorphology, 22(2): 193–204.

Hesse R. 2008. Do swarms of migrating barchan dunes record paleenvironmental changes? A case study spanning the middle to late Holocene in the Pampa de Jaguay, southern Peru. Geomorphology, 104(3–4): 185–190.

Howard A D, Morton J B, Mohamed G. 1978. Sand transport model of barchan dune equilibrium. Sedimentology, 25(3): 307–338.

Kocurek G, Townsley M, Yeh E, et al. 1992. Dune and dune-field development on Padre Island, Texas, with implications for interdune deposition and water-table-controlled accumulation. Journal of Sedimentary Research, 62(4): 622–635.

Landsberg S Y. 1956. The orientation of dunes in Britain and Denmark in relation to wind. Geographical Journal, 122(2): 176–189.

Leithold L. 1992. Calculus, Integral and Analytic Geometry, Volume II (Part I) (3rd ed.). In: Behzad M, Razaghi M, Kazemi S, et al. Tehran: Tehran University Press, 375.

Lettau K, Lettau H. 1969. Bulk transport of sand by the barchans of the Pampa de La Joya in Southern Peru. Geomorphology, 13(2): 182–195.

Mousavi S H, Dorgouie M, Vali A A, et al. 2010. Statistical modeling of morphological parameters of barchan dunes (Case study: Chah Jam Erg in South of Haj Ali GHoli Playa, in Central Part of Semnan Province, IRAN). Journal of Geography and Geology, 2(1): 98–113.

Sauermann G, Rognon P, Poliakov A, et al. 2000. The shape of the barchan dunes of Southern Morocco. Geomorphology, 36(1–2): 47–62.

Tsoar H, Parteli E J R. 2016. Bidirectional winds, barchan dune asymmetry and formation of seif dunes from barchans: a discussion. Environmental Earth Sciences, 75(18): 1237, doi: 10.1007/s12665-016-6040-4.

Wippermann F K, Gross G. 1986. The wind-induced shaping and migration of an isolated dune: A numerical experiment. Boundary-Layer Meteorology, 36(4): 319–334.

Wang Z T, Tao S C, Xie Y W, et al. 2007. Barchans of Minqin: Morphometry. Geomorphology, 89(3–4): 405–411.

Yang J H. Dong Z B. Liu Z Y, et al. 2019. Migration of barchan dunes in the western Quruq Desert, northwestern China. Earth Surface Processes and Landforms, 44(10): 2016–2029.

Zhang Z C, Dong Z B, Hu G Y, et al. 2018. Migration and morphology of asymmetric barchans in the Central Hexi Corridor of northwest China. Geosciences, 8(6): 204, doi: 10.3390/geosciences8060204.